I.A.U. Karaj Branch

*Journal of Applied Chemical Research, Special issue, 119-129 (2015)*

Journal of Applied Chemical Research

www.jacr.kiau.ac.ir

# The Influence of Ag Doping on Structural, Optical Properties and Photocatalytic Activity of $TiO_2/SiO_2$ Nanocomposite

**Bahar Khodadadi**

*Department of Chemistry, University of Qom, Qom, Iran.*

*(Received 12 Nov. 2015; Final version received 16 Dec. 2015)*

**Abstract**

In the present study, $TiO_2/SiO_2$ and $TiO_2/SiO_2$/Ag nanocomposite powders were synthesized by sol-gel technique. Moreover, for investigation of the Ag doping effect different concentrations of dopant were added. Structures were characterized by IR spectroscopy, Scanning Electron Microscopy (SEM), Energy Dispersive Analytical X-Ray (EDAX), and X-Ray Diffraction (XRD) methods. Furthermore, the absorption coefficients of the samples were analyzed by Tauc's model and the direct band gaps were calculated. Photocatalytic activity of all samples was investigated under UV irradiation in an aqueous medium. The results were shown that photocatalytic activity improves in the presence of appropriate amount of Ag as dopant.

***Keywords:*** *Nanocomposite, Sol-Gel technique, Photocatalytic activity, $TiO_2/SiO_2$/Ag.*

## Introduction

The removal of organic pollutants such as dyes which used in textile industry in wastewater is an important method in environmental protection. It is estimated that approximately 15–20% of synthetic textile dyes is lost in wastewater streams during manufacturing or processing operations. The release of these dyes into the environment is harmful because of toxic and mutagenic properties of many dyes. Therefore, textile plant effluents are one of the major water pollutants to the environment. However, the decolorization and degradation of dyes from textile wastewater is still a pertinent issue since these dyes are relatively resistant to conventional biological treatment methods [1-3].

Many methods, including biosorption, conventional activated sludge treatment process [4], electrochemical technologies

***Corresponding author:** Bahar Khodadadi, Department of Chemistry, University of Qom, Qom, Iran. E-mail: bkhodadadi98@yahoo.com, Tel.: +98 25 3210 3792, Fax: +98 25 32850953.*

[5] and reverse osmosis have been applied on wastewater treatment. Photocatalysis has been given universal attention in environment treatment and titanium dioxide ($TiO_2$) are well-known semiconductor that has shown merits of high photosensitivity, non-toxic nature, low cost, and environmentally friendly features for photocatalytic applications [6].However, the band gap energies are large (about 3.2 eV), which means that this semiconductors can only be excited for photocatalytic uses under UV light illumination. However, since UV light accounts for only a small fraction (5%) of the sun's energy compared to visible light (45%), the technological use of $TiO_2$ is largely impaired [7]. Recently, many researchers have reported replacing $TiO_2$ by the $TiO_2/SiO_2$ catalyst, which is an advanced material for self-cleaning and photocatalytic properties, since $TiO_2/SiO_2$ exhibits different surface chemical and photochemical properties compared to $TiO_2$ [8]. However, a good way to enhance the activity of TiO2/SiO2 photocatalyst is through the addition of small amounts of metals, and Ag is one of the best candidates for a dopant because of their novel effects on the improvement of photocatalytic activity of semiconductor [9].

Such enhancement in activity has been explained in terms of a photoelectrochemical mechanism in which the electrons generated by light irradiation of the semiconductor transfer to the loaded metal particles, while the holes remain in the semiconductors, resulting in a decrease in the electron–hole recombination [10].

It has been demonstrated that the structural and morphological characters such as the size, shape, crystalline form, photocatalytic activity and some relevant properties of synthesized samples can be significantly affected by different synthesis methods [11]. Various methods which mainly include template method, precipitation, gas-phase reaction, hydrothermal synthesis and microwave heating have been developed to prepare $TiO_2/SiO_2$ photocatalyst with special performance [12-14].

Among all of synthesis methods, the sole-gel process because of good homogeneity, ease of composition control, low processing temperature, large area coatings, low equipment cost and good optical properties is particularly attractive [15]. In recent years, a few experimental studies have been reported on synthesis via sol-gel method and properties of Ag doped $TiO_2/SiO_2$ nanofilm. Because, sol-gel method mostly used for preparation of nanofilm. In this work, in order to investigation of the influence of Ag doping level on the optical, structural, morphological, and photocatalytic properties of $TiO_2/SiO_2$ nanopowder, $TiO_2/SiO_2$ nanostructure and Ag doped $TiO_2/SiO_2$ nanopowder (with different weight ratio), synthesized via the sol-gel method. Moreover, polyvinyl

pyrrolidone (PVP) is used as organic polymer for preventing agglomeration of nanopowders and modifying photocatalytic activity. The absorption spectra of the samples were measured; the variation of the optical band gap was analyzed. Morphology and samples structure were investigated by IR spectra, Scanning Electron Microscopy (SEM), and X-Ray Diffraction (XRD) methods.

## Experimental

*Materials and Apparatus*

Titanium tetra isopropoxide (TTIP) (AR analytical grade, Merck Chemical Company) was used as a Titanium source for the preparation of the $TiO_2$ photocatalysts. Silver (I) Nitrate, 6 $H_2O$, Polyvinyl pyrrolidone (PVP), $HNO_3$, $SiO_2$ colloid solution, and absolute ethanol, were purchased from Merck Chemical Company. The samples structure were characterized by X-ray diffraction pattern recorded on a Philips model X' PertPro diffractometer employing Cu Kα radiation(λ=1.5418Å) while the morphologies of the synthesized samples were investigated by field emission scanning electron microscopy(FESEM;TESCAN-MIRA3) equipped with an Oxford Inca Energy Dispersive X-ray detector. UV-Visspectra were recorded by using a Shimadzu UV-2500spectrophotometer in the wavelength range 200-700nm. Fourier transform infrared (FT-IR) spectra were obtained using the FT-IR (Jasco, 4200) with the KBr method.

*Sample Preparation*

In a typical procedure, samples were prepared by the Sol-Gel method using the following procedure: First of all, 0.2g PVP was dissolved in absolute ethanol and was stirred 10 min under homogenizer, then TTIP (with molar ratio TTIP/ethanol = 1/75) was dissolved in this solution (solution **I**). Second,HNO3, deionized water, and SiO2(with molar ratio ethanol /$HNO_3$/$H_2O$/$SiO_2$ = 43/0.2/1/30) were dissolved in absolute ethanol (solution **II**). Thirdly, Solution **II** was added drop by drop into solution **I** and vigorously stirred for 30 min at room temperature. The obtained transparent colloidal suspension was sonicated for 30 min, and aged for 48 h to form a gel. The sample was dried in an oven at 50◦C and ultimately calcinated at 500◦C for 4 hours.

Other samples (Ag doped $TiO_2$/$SiO_2$) was prepared exactly similar to same procedure but several concentrationsof AgNO30.5, 1, and 3W/W Ag $NO_3$/ $SiO_2$ were added to solution **II**.

## Results and discussion

*Structural analysis*

Fourier transforming infrared (FTIR) spectroscopy was performed at room temperature in the range of 4000–400 $cm^{-1}$ wave number with the composite powder and the results are shown in Fig. 1.It has been reported that, in all samples, wide absorption

bands were observed around 3100-3700 $cm^{-1}$, due to the OH stretching vibration of surface hydroxyl group because of a great amount of propanol present during the hydrolysis of TTIP [16].Moreover, physically adsorbed water and hydroxyl group causes absorption bands were observed around 1635 $cm^{-1}$ [17].

The bands at 1117 $cm^{-1}$ in samples correspond to asymmetric stretching vibration of the Ti-O bands[18-20] and the ones at around 1070–1075 $cm^{-1}$ are due to the symmetrical vibration of the Si-O-Si bands [19-21]. The peak at 600 $cm^{-1}$ can be assigned to symmetric stretching vibration of the Ti–O–Ti group [22]. Exhibited broad peaks in the range of 400–1000 $cm^{-1}$ have contributions from the anatase phase [20-22].

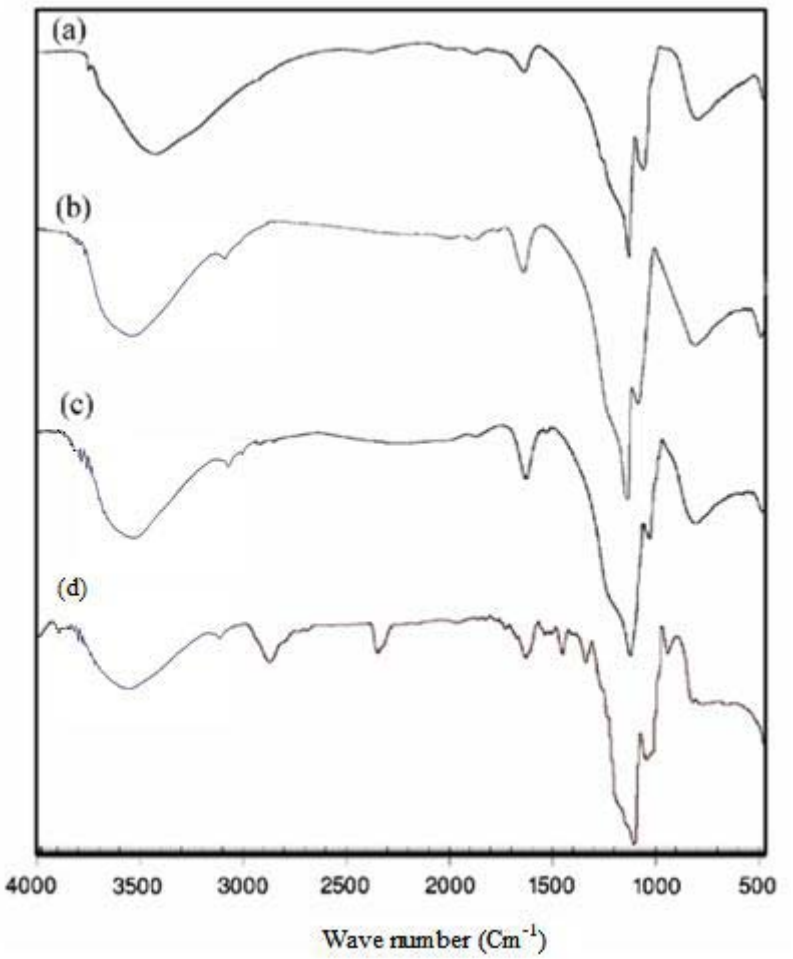


**Figure 1**. FT-IR spectra of the samples (a)$TiO_2/SiO_2$, (b) $TiO_2/SiO_2$/Ag (0.5%), (c) $TiO_2/SiO_2$/Ag (1%),(d) $TiO_2/SiO_2$/Ag (3%).

The crystalline structures of all the synthesized samples were examined by X-ray diffraction (XRD) analysis and results have been shown in Figure 2.

The diffraction patterns of $TiO_2/SiO_2$ sample are well matches with JCPDS card of $TiO_2$ (No. 01-080-0074).This pattern of samples can be indexed to those of anatase structure phase (the base peak in range of 20<**2θ**<30 is an evidence of anatase phase). Moreover, diffraction peaks at 25.3, 37.8, 48.2, 55.1, 62.9, 70.5, and 82.9 assigned to the characteristic anatase phase and diffraction peaks at 27.5, 36.2, 41.5, 45.2, 54.5, 57, and 69.5 assigned to the characteristic rutile phase[23]. In the meantime, XRD patterns for all of samples showed both anatase and rutile phase, but anatase phase was dominated.

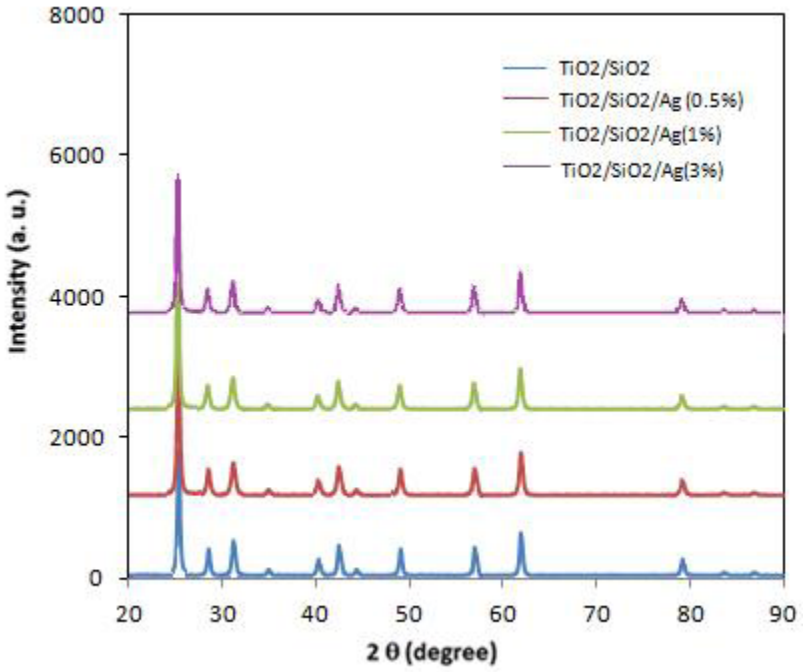


**Figure 2**. XRD patterns of sol-gel synthesized samples.

On the basis of the results, in comparison with the spectrum of $TiO_2/SiO_2$, while the samples doped with different concentration of Ag results indicate that the samples were single phase with $TiO_2$ without a formation of impurities like $Ag_2O$. However, it should be noted that the metallic Ag phase cannot be detected in the samples due to a low concentration [24]. The diffraction peaks of $TiO_2/SiO_2$/Ag samples were shifted to lower angles with the increasing Ag concentration. The shift of peaks to lower values was reasonable because the ionic radius of $Ag^+$(0.122 nm) is larger than that of $Zn^{2+}$ (0.060 nm)implies that silver ions

diffused into the lattice of $TiO_2$ [25]. Moreover, the mean crystallite size was calculated using the Scherrer equation[26]:

$$D = k\lambda/\beta\cos\theta$$

Where λ is the wavelength of X-ray radiation, K is usually 0.89 is the Scherrer constant, λ= 1.5418 Å is the wavelength of the X-ray radiation, β is the peak full width at half maximum in radians and θ is the Bragg diffraction angle. The estimated values of grain size are in 25-30 nm range. The results are summarizes in Table 1.

**Table 1**. Peak position, band gap, and mean crystal size of samples.

| Sample | (101) Peak position (degree) | Mean Crystal Size (nm) | Wavelength (nm) | Bandgap (eV) |
|---|---|---|---|---|
| $TiO_2/SiO_2$ | 25.4122 | 28.63 | 390 | 2.82 |
| $TiO_2/SiO_2$/Ag(0.5%) | 25.3419 | 27.57 | 391 | 2.77 |
| $TiO_2/SiO_2$/Ag (1%) | 25.2182 | 26.59 | 392 | 2.72 |
| $TiO_2/SiO_2$/Ag (3%) | 25.1795 | 25.79 | 395 | 2.64 |

All samples were identified by Scanning Electron Microscopy (SEM) analysis and according to results, in all samples; nanoparticles are relatively uniform and global. The composition of samples was determined by the elemental dispersion analysis using X-ray (EDAX) measurements. The EDAX results for samples confirm the presence and uniform distribution of the elements Ti, Si, O and Ag. Fig. 3 illustrates a typical SEM image and EDAX analysis of the $TiO_2/SiO_2$/Ag (1 %) sample.

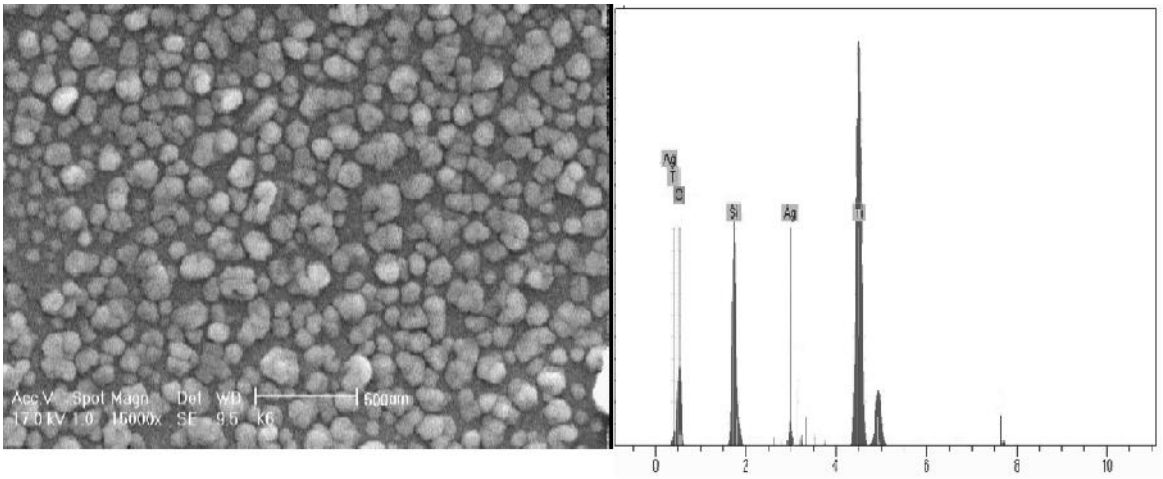


**Figure 3**. SEM image and EDAX analysis of $TiO_2/SiO_2$/Ag (1%) sample.

*Optical Properties*

The optical properties of the samples, as measured by UV–Vis diffuse reflection spectrophotometer at room temperature, are displayed in Fig. 4. It can be seen that, in all of samples, the absorption edge around 390 nm belongs to the intrinsic exciton absorption of $TiO_2$.

It can be clearly seen that the maximum of the absorbance band shifts slightly toward higher wavelength due to Ag doping and sample $TiO_2$/$SiO_2$ contain 3% Ag shows huge absorption intensity in higher wavelength region (Table 1).

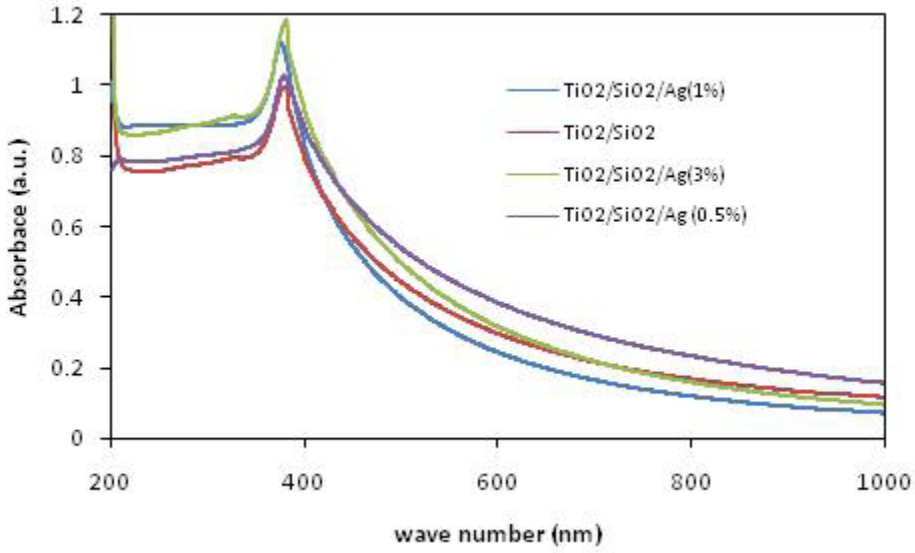


**Figure 4**. UV-Vis spectrum of samples.

The absorption coefficients of the samples are analyzed by Tauc's approach [27], and the direct band gap is calculated using the following equation:

$$\alpha = C\,(h\nu - E_g^{bulk})^2 / h\nu$$

Where α is the absorption coefficient, C is a constant, hν is the photon energy and $E_g$ bulk is the band gap. Figure 5 shows the Tauc plots of samples. Extrapolation of the linear region of Tauc plot gives a band gap. From Figure 5 and Table 1, it can be seen that, compared with $TiO_2$/$SiO_2$ sample, the band gap of the samples with dopant slightly decreases with increase in dopant concentration. It seems that, existence of Ag ions impurities in the $TiO_2$ structure, induce the formation of new recombination centers with lower emission energy and cause the narrowing band gap energy [28].

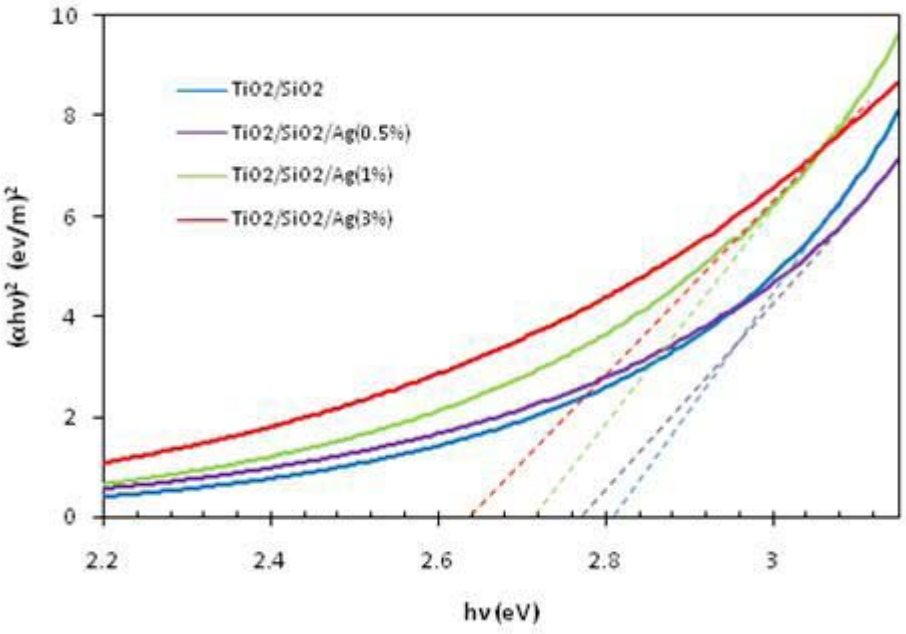


**Figure 5.** The Tauc plots of samples.

Evaluation of Photocatalytic Activity

For investigation of photocatalytic activity of the samples and the effect of Ag doping on photocatalytic activity, several solutions of Methylene blue (5 $mgL^{-1}$) in deionized water were selected as pollutant solutions for photodegradation. These solutions were set in the vicinity of a nano photocatalyst powder (0.2 g powder in 1L solution) and then placed in the darkness for 24 hin order to eliminate the absorptive effect of the solution in the catalyst. Finally, the solutions were placed in the photoreactor and Methylene blue (MB) concentration change was recorded by UV spectroscopy. This photoreactor system consisted of a cubic borosilicate glass reactor with an effective volume of 1000 mL, a cooling water jacket and a 15W UV lamp (Osram) with a quartz cover positioned inside the solution used as a UV light source. The reaction temperature was kept at 25 ºC using cooling water. Fig. 6 shows the photocatalytic degradation curves of MB in presence of samples. It can be found that the degradation ratio of MB is increased gradually with an increase in the Ag dopant content.

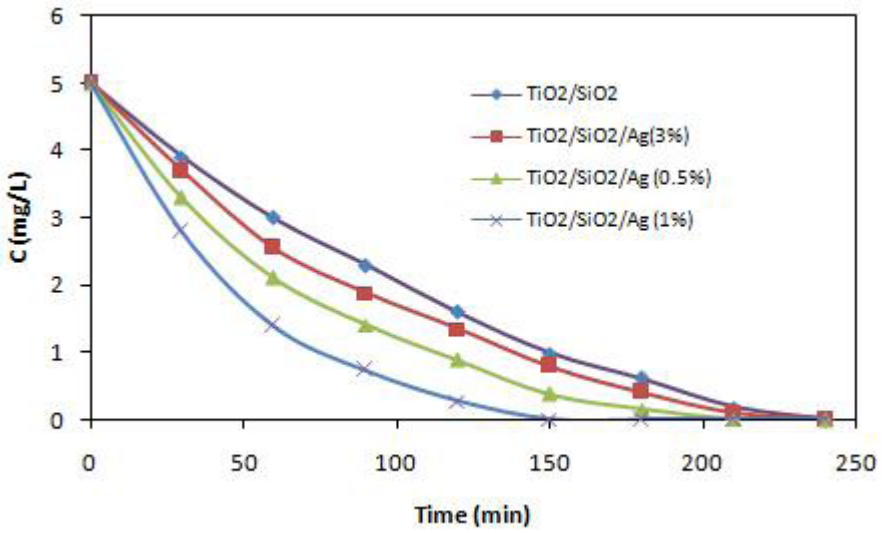


**Figure 6**. Photodegradation of methylene blue (MB) using the samples.

It is worth noting that, the semiconductor photocatalysis is based on the generation of electron (e-) –hole (h+) pair upon UV light irradiation. The electron can be migrated from the valence band to the conduction band, leaving behind hole in the valence band [29]. Based on the above results, increasing of the photocatalytic activity of which may be due to the presence of the appropriate amount of Ag species on the surface layer of TiO2can effectively capture the photoinduced electrons and holes. Moreover, photoinduced electrons can quickly transfer to the oxygen adsorbed on the surface of TiO2. Consequently, sample contain 1% Ag as dopant, exhibited more effective electron–hole separation under UV–Vis light irradiation since and more photocatalytic activity in comparison with other samples. However, when the Ag content exceeds 1%, the number of active sites capturing the photoinduced electron is decreased and, excessive Ag can cover the surface of TiO2, leading to a decrease in the concentration of photogenarated charge carrier and photocatalytic activity of photocatalyst [27-29].

## Conclusion

This research has verified that the photocatalytic activity of $TiO_2/SiO_2$ nanocomposite powder can be improved using metal doping. All samples have been prepared bysol–gel method and PVP has been used as modifier. Furthermore, XRD pattern confirmed that anatase structure in all of samples is dominant phase. UV–Vis diffuse reflectance spectroscopy showed red shift with Ag doping. Moreover, the absorption coefficients of samples were analyzed by Tauc's approach and calculations confirmed

that application of dopant and dopant concentration are very effective on band gap. The photocatalytic activity of the samples was examined for degradation of methylene blue in water under UV irradiation in a batch reactor. The results revealed that the photocatalytic activity of the nanocomposites has increased in the presence of Ag and according to other results; the sample with 1% Ag exhibited the best photocatalytic activity.

**References**

[1] C.E. Clarke, F. Kielar, H.M. Talbot, K.L. Jouhnson, *Environ. Sci. Technol*., 44, 1116 (2010).

[2] C.S. Pan,Y.F. Zhu, *Environ. Sci. Technol*., 44, 5570 (2010).

[3] H.Y. Zhu, L. Xiao, R. Jiang, G. M. Zeng,L. Liu, *J. Chem. Eng.*, 172, 746 (2011).

[4] A. Katsoyiannis, C. Samara, *Environ. Res*., 97, 245 (2005).

[5] D. Rajkumar,K. Palanivelu, *J. Hazard. Mater.,* 113, 123 (2004).

[6] F. Peng,Y.Q. Ren, *Chin. J. Catal*., 24, 243 (2003).

[7]F. Peng, H. Wang, H. Yu, Sh. Chen, *Mater. Res. Bull*., 41, 2123 (2006).

[8] Z. Liu, X. Zhang, T. Murakami, A. Fujishima, Sol. Energy Mater. *Sol. Cells*., 92, 1434 (2008).

[9] P. Amornpitoksuk , S. Suwanboon , S. Sangkanu , A. Sukhoom , N. Muensit , J. Baltrusaitis, *Powder Technol*., 219,158 (2012).

[10] J. C. Sin, S. M. Lam, K. T. Lee, A. R. Mohamed, *Ceram. Int*., 39, 5833 (2013).

[11] W.D. Yu, X.M. Li, X.D. Gao,F. Wu, *J. Phys. Chem. B.,* 109, 17078 (2005).

[12] G. Colon, M.C. Hidalgo, J.A. Navio, E.P. Melian, O.G. Diaz, J.M. Rodriguez, *Appl. Catal. B: Environ*., 83, 30 (2008).

[13] I.A. Siddiquey, T. Furusawa, M. Sato, N. Suzuki, *Mater. Res. Bull*., 43, 3416 (2008).

[14] J. H. Sun, S. Y. Dong, J. L. Feng, X. J. Yin, X. C. Zhao,*J. Mol. Catal. A: Chem*., 335, 145 (2011).

[15] J. Zhong, J. Z. Li, X. Y. He, J. Zeng, Y. Lu, W. Hu, K. Lin, *Curr. App. Phys*., 12, 998 (2012).

[16]M.P. Zheng, M. Gu, Y. Jin, G. Jin, *J. Mater. Sci. Eng. B*.,77, 55 (2000).

[17] K.M. Parida, N. Sahu, *J. Mol. Catal. A: Chem.*, 287, 151 (2008).

[18] M.P. Zheng,M.Y. Gu, Y.P. Jin, H.H. Wang, P.F. Zu, P. Tao, J.B. He, *J. Mater. Sci. Eng. B*.,87, 197 (2001).

[19] J. Jiao, Q. Xu, L. Li, *J. Colloid Interface Sci*.,316, 596 (2007).

[20] M. Houmard, D. Riassetto, F. Roussel, A. Bourgeois, G. Berthome, J.C.Joud, M. Langlet, *J. Surf. Sci.,* 602, 3364 (2008).

[21]B.Khodadadi,M.Sabeti,B.Nahri-Niknafs, S. Moradi-Dehaghi, P. AberomandAzar, S. Raeis Farshid, *Bug. Chem. Chemmun*., 46, 624 (2014).

[22] B. Khodadadi; M. Sabeti, S. Moradi, P. Aberomand Azar, S. Raies Farshid, *J. Appl.*

*Chem. Res*.,20, 36 (2012).

[23]L. Zhang, X. Li, Z. Chang,D. Li, *Mat. Sci. Semicon. Proc.,* 14, 52 (2011).

[24] R. Liu, P. Wang, X. Wang, H. Yu, J. Yu, *J. Phys. Chem. C.*, 116, 17721 (2012).

[25] B. Xin, L. Jing, Z. Ren, B. Wang, H.Fu, *J. Phys. Chem. B*., 109, 2805(2005).

[26] A. Patterson., *Phys. Rev*., 56, 978 (1939).

[27] H. Fu, C. Pan, W. Yao, Y. Zhu, *J. Phys. Chem. B.,*109, 22432 (2005).

[28] R. Mohana, K. Krishnamoorthy, S. Kima, *Solid State Commun*., 152, 375 (2012).

[29] Y.H. Zheng, C.Q. Chen, Y.Y. Zhan, X.Y. Lin, Q. Zheng, K.M. Wei, J.F. Zhu,Y.J. Zhu, *Inorg. Chem*., 46, 6675 (2007).